Let us check the functionals (39) and (40) by studying their special cases for the isotropic guide, i.e., for $\xi = \zeta = 0$. Writing $\bar{\bar{L}} = (\mu\epsilon - v_p^2)I_t$ and $M^T = M$, we have

$$J(v_p; f) = \frac{\int_S \frac{1}{\mu\epsilon - v_p^2}\left[\nabla f^* \cdot M\nabla f + \frac{1}{v_p}\nabla f^* \cdot J\boldsymbol{u}_z \times \nabla f\right] dS}{\int_S f^* M f\, dS}$$

$$= \frac{\int_S \frac{1}{\mu\epsilon - v_p^2}\left[\epsilon|\nabla e|^2 + \mu|\nabla h|^2 + \frac{2}{v_p}\Re\{\boldsymbol{u}_z \cdot \nabla e \times \nabla h^*\}\right] dS}{\int_S (\epsilon|e|^2 + \mu|\mu|^2)\, dS}. \tag{41}$$

This expression can be seen to coincide with that given in [10] (note that the factor $1/v_p$ in the (21) of the referenced paper is erroneously missing).

III. Discussion

The functional (39) is exact and presents an obvious extension of previously known functionals from isotropic to bi-isotropic media. It can be applied to obtaining approximate mode solutions for open bi-isotropic waveguides. By approximating the longitudinal field functions, the dispersion function $\beta(\omega)$ can be obtained point by point. In practice, this can be performed using the following scheme:

1. Choose a value for the phase velocity parameter v_p.
2. Find suitable approximating functions for the longitudinal fields $e(\boldsymbol{\rho})$ and $h(\boldsymbol{\rho})$, i.e., the matrix $f(\boldsymbol{\rho})$, with free parameters. Insight on the field distribution of the problem will help in allowing use of just a few parameters; otherwise, a massive computation scheme with a great number of parameters is needed.
3. Optimize values of these parameters so that the functional $J(v_p; f)$ obtains the stationary value; i.e., its differentiation with respect to all these parameters is zero. (In case of large number of parameters this requires use of some optimization procedure.)
4. The corresponding parameter values inserted in the longitudinal field expressions give closest approximations to the fields and the functional value approximates the value of ω^2.
5. Now it is easy to determine a point on the dispersion diagram: $\omega = \sqrt{\omega^2}$, $\beta = \omega v_p$.
6. The transverse field functions corresponding to this point are obtained from (23).
7. To find another point, start with another value of v_p.

Thus, the procedure works best when some *a priori* knowledge of the longitudinal fields exists, which helps in finding suitable approximating functions with not too many optimizable parameters. Obviously, the method is especially attractive for finding the lowest-order modes with least spatial variation. To find the knowledge required, it appears necessary to work through some examples with brute-force technique. This is, however, outside the scope of the present theoretical study.

References

[1] D. L. Jaggard, J. C. Liu, and X. Sun, "Spherical Chiroshield," *Electron. Lett.*, vol. 27, no. 1, pp. 77–79, Jan. 1991.

[2] I. V. Lindell, A. H. Sihvola, A. J. Viitanen, and S. A. Tretyakov, "Geometrical optics in inhomogeneous chiral media with applications to polarization correction in inhomogeneous lens antennas," *J. Electromagn. Waves Appl.*, vol. 4, no. 6, pp. 533–548, 1990.

[3] N. Engheta and P. Pelet, "Reduction of surface waves in chirostrip antennas," *Electron. Lett.*, vol. 27, no. 1, pp. 5–7, Jan. 1991.

[4] A. Lakhtakia, V. K. Varadan, and V. V. Varadan, *Time-Harmonic Electromagnetic Fields in Chiral Media*. Berlin: Springer, 1989.

[5] B. D. H. Tellegen, "The Gyrator, a new electric network element," *Philips Res. Rep.*, vol. 3, pp. 81–101, 1948.

[6] J. C. Monzon, "Radiation and scattering in homogeneous general biisotropic regions," *IEEE Trans. Antennas Propagat.*, vol. 38, no. 2, pp. 227–235, Feb. 1990.

[7] I. V. Lindell and A. J. Viitanen, "Duality transformations for general bi-isotropic (nonreciprocal chiral) medium," *IEEE Trans. Antennas Propagat.*, vol. 40, no. 1, Jan. 1992.

[8] I. V. Lindell, "Variational methods for nonstandard eigenvalue problems in waveguide and resonator analysis," *IEEE Trans. Microwave Theory Tech.*, vol. MTT-30, no. 8, 1194–1204, August, 1982.

[9] I. V. Lindell and A. H. Sihvola, "Dielectrically loaded corrugated waveguide: variational analysis of a nonstandard eigenproblem," *IEEE Trans. Microwave Theory Tech.*, vol. MTT-31, no. 7, pp. 520–526, July 1983.

[10] I. V. Lindell and M. I. Oksanen, "Transversely anisotropic optical fibers: variational analysis of a nonstandard eigenproblem," *IEEE Trans. Microwave Theory Tech.*, vol. MTT-31, no. 9, pp. 736–745, September 1983.

[11] W. X. Zhang, *Engineering Electromagnetism: Functional Methods*. London: Ellis Horwood, 1991.

Analysis of Bilateral Fin-Lines on Anisotropic Substrates

Thinh Quoc Ho and Benjamin Beker

***Abstract*—A full-wave analysis of the bilateral fin-line on anisotropic substrates is presented. The supporting medium is characterized simultaneously by both nondiagonal second rank [ϵ] and [μ] tensors. The dyadic Green's function is formed rigorously in the discrete Fourier transformed domain and is used to study the propagation characteristics of the fin-line. The Green's function elements are given explicitly in their closed forms along with the verification of the theory. New data describing the dispersion properties as functions of the coordinate misalignment are also generated for several substrate materials.**

I. Introduction

Although the theories of transmission lines on anisotropic structures are well documented, the major effort thus far has been di-

Manuscript received June 3, 1991; revised October 4, 1991.

The authors are with the Department of Electrical and Computer Engineering, University of South Carolina, Columbia, SC 29208.

IEEE Log Number 9104773.

rected toward structures whose substrates are characterized by a diagonalized $[\epsilon]$ tensor only. A review of the treatments to those problems outlining the procedure for the study of the propagation characteristics of various transmission lines may be found in [1]–[3]. In practice, however, most of the above analyses are somewhat limited in scope due to the absence of the off-diagonal elements in the permittivity tensor, which may be used to represent the misalignment between the material coordinate system and that of the waveguide, as indicated in [4]. In addition, the response to the magnetic fields for the aforementioned cases is normally assumed to be isotropic, that is, when $[\mu]$ is specified as a zero-rank tensor (scalar). For problems involving transmission lines on general anisotropic substrates, that is, when the materials are characterized by both permittivity and permeability tensors, the solution to Maxwell's equations required for the study of their propagation characteristics, can no longer be obtained in a straight forward manner. Up until now, there are only a few publications [5]–[8] which have reported some research efforts dealing with transmission lines whose substrate material is characterized simultaneously by both $[\epsilon]$ and $[\mu]$ tensors. The fact that the shielded transmission lines on a general anisotropic media have not yet received full attention, as did their counterparts printed on substrates characterized by $[\epsilon]$ tensor alone, provides the motivation for this work.

The purpose of this paper is to present the analysis of bilateral fin-lines on general anisotropic substrates. In this study, unlike some others conducted in the past, both $[\epsilon]$ and $[\mu]$ tensors are nondiagonal. As a result, the Green's function derived herein may be used to examine the dispersion properties of the structure on both dielectric and magnetic substrates. The bilateral fin-line is selected mainly due to its popularity in applications at millimeter-wave frequencies. Also, this type of a transmission line does not support a TEM-like mode. It has a cut off at lower frequencies, and as such is fundamentally different from other transmission lines. At the present time, there is no comprehensive treatment of this structure that is printed on the type of anisotropic materials considered in this study. Consequently, the aim of this work is to present the analytical tools which can be used in the analysis of bilateral fin-lines whose substrates can exhibit a wide variety of anisotropic properties.

II. Theory

The cross section of the bilateral fin-line is shown in Fig. 1 along with the coordinate system used in the analysis. The millimeter-wave circuit using the fin-line is usually excited by a dominant TE_{10} mode of the rectangular waveguide having dimensions a and b. The direction of propagation of the resulting wave is along the z-axis. In this geometry, the gap that separates the metal fins is denoted as W. The supporting substrate onto which the fins are mounted is suspended along the E-plane of the waveguide, and is specified by

$$[\epsilon] = \epsilon_o \begin{vmatrix} \epsilon_{xx} & \epsilon_{xy} & 0 \\ \epsilon_{yx} & \epsilon_{yy} & 0 \\ 0 & 0 & \epsilon_{zz} \end{vmatrix} \tag{1a}$$

$$[\mu] = \mu_o \begin{vmatrix} \mu_{xx} & \mu_{xy} & 0 \\ \mu_{yx} & \mu_{yy} & 0 \\ 0 & 0 & \mu_{zz} \end{vmatrix} \tag{1b}$$

where ϵ_o and μ_o denote the free-space values of permittivity and permeability, respectively.

To determine the types of solutions for the electromagnetic fields,

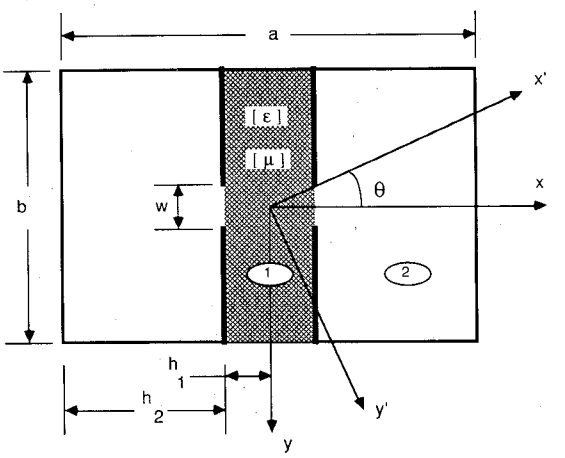

Fig. 1. Geometry of the bilateral fin-line on a general anisotropic substrate.

that may exist within the planar anisotropic region, the two curl equations are employed. It can be shown that the vector wave equations for all components of the electric and magnetic fields may be written compactly in the form of

$$\nabla \mathrm{X}([\mu]^{-1} \cdot \nabla \mathrm{X} \boldsymbol{E}) - k_o^2[\epsilon] \cdot \boldsymbol{E} = 0 \tag{2a}$$

$$\nabla \mathrm{X}([\epsilon]^{-1} \cdot \nabla \mathrm{X} \boldsymbol{H}) - k_o^2[\mu] \cdot \boldsymbol{H} = 0 \tag{2b}$$

where k_o is the free-space wave number.

To obtain the field solutions within the anisotropic medium, either the wave equation for $\boldsymbol{E}$ or the wave equation for $\boldsymbol{H}$ may be used. It is more convenient to work with the wave equation for the electric field mainly because the problem involves several electric ground planes which belong to the housing. Consequently, the vector wave equation for the electric field may be reduced to three scalar equations which can be written in terms of the electric field components alone. The process of separating (uncoupling) these equations to get a set of independent equations for individual components of the E-field begins with their transformation to the Fourier domain.

The spectral representation of any field component is defined via the following transform:

$$\tilde{\Psi}(x, \alpha) = \int_{-b/2}^{b/2} \Psi(x, y) e^{j\alpha y}\, dy \tag{3}$$

where $\alpha = n\pi/b$ is the discrete transform variable. As a result, the three scalar equations for the components of the electric field are transformed into the Fourier-domain according to definition (3). With the help of the divergence equation, $\tilde{E}_x$ is eliminated, yielding a set of two coupled equations for $\tilde{E}_y$ and $\tilde{E}_z$. In general, the coupled equations may be expressed in terms of any two field components. However, in this formulation, the two components that are chosen are $\tilde{E}_y$ and $\tilde{E}_z$. With that choice, the coupled differential equations for $\tilde{E}_y$ and $\tilde{E}_z$ can be shown to satisfy

$$\frac{\partial^2 \tilde{E}_y}{\partial x^2} + Y_1 \frac{\partial \tilde{E}_y}{\partial x} + Y_2 \tilde{E}_y + Y_3 \frac{\partial \tilde{E}_z}{\partial x} + Y_4 \tilde{E}_z = 0 \tag{4a}$$

$$\frac{\partial^2 \tilde{E}_z}{\partial x^2} + Z_1 \frac{\partial \tilde{E}_z}{\partial x} + Z_2 \tilde{E}_z + Z_3 \frac{\partial \tilde{E}_y}{\partial x} + Z_4 \tilde{E}_y = 0 \tag{4b}$$

with their coefficients given by

$$Y_1 = -j\alpha\epsilon_{xy}/\epsilon_{xx} + j\alpha Y_o'/\mu_{zz} \tag{5a}$$

$$Y_o = \{k_o^2\epsilon_{yx}\mu_{zz} - \alpha^2\epsilon_{yx}/\epsilon_{xx} - \beta^2\mu_{xy}\mu_{zz}/\mu_d\} \{-k_o^2\epsilon_{xx} + \alpha^2/\mu_{zz} + \beta^2\mu_{xx}/\mu_d\}^{-1} \quad (5b)$$

$$\mu_d = \mu_{xx}\mu_{yy} - \mu_{xy}\mu_{yx} \quad (5c)$$

$$Y_2 = \{k_o^2\epsilon_{yy}\mu_{zz} - \alpha^2\epsilon_{yy}/\epsilon_{xx} - \beta^2\mu_{yy}\mu_{zz}/\mu_d - (\beta^2\mu_{yx}/\mu_d - k_o^2\epsilon_{xy})Y_o\} \quad (5d)$$

$$Y_3 = j\beta\mu_{zz}\mu_{xy}/\mu_d + j\beta\mu_{xx}Y_o/\mu_d \quad (5e)$$

$$Y_4 = \alpha\beta\mu_{yy}\mu_{zz}/\mu_d - \alpha\beta\epsilon_{zz}/\epsilon_{xx} + \alpha\beta\mu_{yx}Y_o/\mu_d \quad (5f)$$

$$Z_1 = -j\alpha\mu_{yx}/\mu_{xx} - j\alpha\mu_{xy}/\mu_{xx} + j\beta\mu_{xx}Z_o/\mu_d \quad (5g)$$

$$Z_o = \{\alpha\beta\mu_{xy}/\mu_{xx} - \alpha\beta\epsilon_{yx}/\epsilon_{xx}\} \{-k_o^2\epsilon_{xx} + \alpha^2/\mu_{zz} + \beta^2\mu_{xx}/\mu_d\}^{-1} \quad (5h)$$

$$Z_2 = \{k_o^2\epsilon_{zz}\mu_d/\mu_{xx} - \alpha^2\mu_{yy}/\mu_{xx} - \beta^2\epsilon_{zz}/\epsilon_{xx} + \alpha\beta\mu_{yx}Z_o/\mu_d\} \quad (5i)$$

$$Z_3 = j\beta\mu_{yx}/\mu_{xx} - j\beta\epsilon_{xy}/\epsilon_{xx} + j\alpha Z_o/\mu_{zz} \quad (5j)$$

$$Z_4 = \alpha\beta\mu_{yy}/\mu_{xx} - \alpha\beta\epsilon_{yy}/\epsilon_{xx} - (\beta^2\mu_{yx}/\mu_d - k_o^2\epsilon_{xy})Z_o. \quad (5k)$$

These coefficients are functions of the medium parameters, transform variable α, k_o, and the propagation constant β which is defined along the z direction.

Decoupling of the above set is possible by the substitution method which after some manipulations leads to yet another, but an independent pair of fourth-order differential equations for these components of the electric field, i.e.,

$$\frac{\partial^4\tilde{E}_y}{\partial x^4} + A\frac{\partial^3\tilde{E}_y}{\partial x^3} + B\frac{\partial^2\tilde{E}_y}{\partial x^2} + C\frac{\partial\tilde{E}_y}{\partial x} + D\tilde{E}_y = 0 \quad (6a)$$

$$\frac{\partial^4\tilde{E}_z}{\partial x^4} + E\frac{\partial^3\tilde{E}_z}{\partial x^3} + F\frac{\partial^2\tilde{E}_z}{\partial x^2} + G\frac{\partial\tilde{E}_z}{\partial x} + H\tilde{E}_z = 0 \quad (6b)$$

where the transformed constants A, B, C, and D are defined below:

$$A = Y_1 - (Y_4 - Y_3Z_1)/Y_3 + \frac{Y_3Z_2 + Y_4(Y_4 - Y_3Z_1)/Y_3}{Y_4 - Y_3(Z_1 - Z_2Y_3/Y_4)} \quad (7a)$$

$$B = Y_2 - Y_3Z_3 - Y_1(Y_4 - Y_3Z_1)/Y_3 + (Y_1 + Y_3Z_2/Y_4) \cdot \frac{Y_3Z_2 + Y_4(Y_4 - Y_3Z_1)/Y_3}{Y_4 - Y_3(Z_1 - Z_2Y_3/Y_4)} \quad (7b)$$

$$C = -Y_3Z_4 - Y_2(Y_4 - Y_3Z_1)/Y_3 + (Y_2 - Y_3Z_3 + Y_3Z_2Y_1/Y_4)\frac{Y_3Z_2 + Y_4(Y_4 - Y_3Z_1)/Y_3}{Y_4 - Y_3(Z_1 - Z_2Y_3/Y_4)} \quad (7c)$$

$$D = -Y_3(Z_4 - Y_2Z_2Y_4)\frac{Y_3Z_2 + Y_4(Y_4 - Y_3Z_1)/Y_3}{Y_4 - Y_3(Z_1 - Z_2Y_3/Y_4)} \quad (7d)$$

and where the coefficients E, F, G, and H are also functions of Y_1, Y_2, Y_3, Y_4, Z_1, Z_2, Z_3, and Z_4. Within a shielded housing, the solutions to (6) are standing waves. In general, these solutions are written in terms of sinusoidal and cosinusoidal functions. Due to the symmetry of the structure, the boundary conditions require the tangential magnetic fields to be zero at the magnetic wall ($x = 0$), reducing the general solutions to having cosine functions only. Subsequently, when the two tangential electric field components have been determined, the remaining field components such as $\tilde{E}_x$, $\tilde{H}_x$, $\tilde{H}_y$, and $\tilde{H}_z$ may be expressed in terms of $\tilde{E}_y$ and $\tilde{E}_z$ through the Maxwell's curl equations. On the other hand, in the isotropic region, the field components may be found by using the scalar potential functions. The procedure for finding them is already available in [9], and therefore, will not be repeated here.

Once all the field components in both regions are known, the Green's function of the structure may be obtained by enforcing the appropriate boundary conditions at the air-substrate interface

$$\tilde{E}_{y1} = \tilde{E}_{y2} \quad (8a)$$

$$\tilde{E}_{z1} = \tilde{E}_{z2} \quad (8b)$$

$$\tilde{H}_{y1} - \tilde{H}_{y2} = -\tilde{J}_z \quad (8c)$$

$$\tilde{H}_{z1} - \tilde{H}_{z2} = \tilde{J}_y \quad (8d)$$

where $\tilde{J}_y$ and $\tilde{J}_z$ are the Fourier transforms of unknown current densities J_y and J_z on the fins at $x = h_1$.

After some mathematical manipulations, the dyadic Green's function in the Fourier transformed domain is found to relate the fields across the slot to the currents on the fins through the following matrix equation:

$$[\tilde{G}]\begin{vmatrix}\tilde{E}_y\\ \tilde{E}_z\end{vmatrix} = \begin{vmatrix}\tilde{J}_{ys}\\ \tilde{J}_{zs}\end{vmatrix} \quad (9)$$

with the expressions for $\tilde{G}_{yy}$, $\tilde{G}_{yz}$, $\tilde{G}_{zy}$, $\tilde{G}_{zz}$ given in the Appendix. Notice that $\tilde{E}_z$ and $\tilde{E}_y$ in the above equations are finite across the slot at $x = h_1$ for $0 < |y| < w/2$, but they are zero on the metal fins. In order to find the numerical solution, the aperture fields are expanded using the known basis functions [9],

$$\tilde{E}_y(n) = \sum_{m=1}^{M} C_m\tilde{E}_{ym}(\alpha(n)) \quad (10a)$$

$$\tilde{E}_z(n) = \sum_{m=1}^{N} D_m\tilde{E}_{zm}(\alpha(n)) \quad (10b)$$

with C_m and D_m being the unknown expansion coefficients. After the appropriate substitutions between (9) and (10) along with the application of the Parseval's theorem in the discrete Fourier domain, the system of matrix equations which is used to extract the propagation constant β is formed:

$$\sum_{m=1}^{M} K_{im}^{(y,y)}C_m + \sum_{m=1}^{N} K_{im}^{(y,z)}D_m = 0 \qquad i = 1, 2, 3, \cdots N \quad (11a)$$

$$\sum_{m=1}^{M} K_{im}^{(z,y)}C_m + \sum_{m=1}^{N} K_{im}^{(z,z)}D_m = 0 \qquad i = 1, 2, 3, \cdots N \quad (11b)$$

with its elements given by

$$K_{im}(p, q) = \sum_{n=0}^{\infty} \tilde{E}_{yp}(n)\tilde{G}_{pq}(n, \beta)\tilde{E}_{yq}(n) \quad (11c)$$

where p or q can be either y or z. The roots which correspond to the propagation constants are found by setting the determinant of the coefficient matrix equal to zero, and solving the resulting equation (11) using the technique described in [9].

III. Results

To validate the newly derived expressions of the Green's function elements, numerical results for the effective dielectric constant ϵ_{eff} (β^2/k_o^2) for two special cases are computed and compared to the existing data. In the first case, the supporting medium is taken to be isotropic with $\epsilon_{xx} = \epsilon_{yy} = \epsilon_{zz} = 3.75$, $\mu_{xx} = \mu_{yy} = \mu_{zz} = 1.0$,

and $\epsilon_{xy} = \epsilon_{yx} = \mu_{xy} = \mu_{yx} = 0$. The chosen housing is a standard WR-28 waveguide, with the remaining dimensions given by $h_1 = 0.0625$ mm, $h_2 = 3.4935$ mm, and $W = 0.5$ mm. For the second case, all physical dimensions of the structure are the same, but the substrate is a dielectrically anisotropic medium with $\epsilon_{xx} = \epsilon_{zz} = 3.0$, $\epsilon_{yy} = 3.5$, $\mu_{xx} = \mu_{yy} = \mu_{zz} = 1.0$, and $\epsilon_{xy} = \epsilon_{yx} = \mu_{xy} = \mu_{yx} = 0$. Fig. 2 shows the effective dielectric constant computed by this method along with the data produced from [2], [9]. The comparison of the results indicates that, in general, the agreement is very good. For the isotropic substrate, the ϵ_{eff} matches very well, including frequencies below the designated bandwidth (26.5 GHz–40.0 GHz). However, for the uniaxial material, a minor discrepancy is observed at frequencies near the cut off point, but otherwise, everywhere else, the agreement is good. This difference in the results near the cut off can probably be attributed to the numerical convergence of the data obtained by the two methods. In all of the calculations presented in this paper, the values of $N = 5$, $M = 5$, and $n = 350$ terms were used to ensure convergence.

Now that the Green's function has been validated, the effects of the nondiagonal elements in the $[\epsilon]$ and $[\mu]$ tensors on the dispersive properties of bilateral fin-lines can be examined. First, the permeability tensor of the substrate is made isotropic by allowing $\mu_{xx} = \mu_{yy} = \mu_{zz} = 1.0$ with μ_{xy} and $\mu_{yx} = 0$. The effective dielectric constant of the fin-line is then studied as a function of the rotation angle θ which in practice may be used to represent the misalignment between the coordinate system of the waveguide and that of the substrate material. This leads to the following definitions for the tensor elements of the permittivity appearing in (1a): $\epsilon_{xx} = \epsilon_2 \sin^2(\theta) + \epsilon_1 \cos^2(\theta)$, $\epsilon_{yy} = \epsilon_2 \cos^2(\theta) + \epsilon_1 \sin^2(\theta)$, $\epsilon_{zz} = \epsilon_3$, and $\epsilon_{xy} = \epsilon_{yx} = (\epsilon_2 - \epsilon_1) \sin(\theta) \cos(\theta)$, where ϵ_1, ϵ_2, and ϵ_3 are the principal values of the $[\epsilon]$ tensor. Numerical results in Fig. 3 show the response of ϵ_{eff} when the fins are printed on the PTFE or glass cloths, both of which are dielectrically biaxial substrates. The effective dielectric constant of the fin-line is computed at frequencies of 26.0 GHz, 33.0 GHz, and 40.0 GHz and is plotted versus the rotation angle θ. As can be seen from this figure ϵ_{eff} becomes larger with increasing frequency, however, for both of the cloth materials it is decreasing, but only slightly, as the angle θ varies from 0 to 90 degrees. This behavior is totally opposite to that of the microstrip line wherein it is found ϵ_{eff} increases with values of the rotation angle changing from 0° to 90°, as illustrated in [10].

Next, the response of ϵ_{eff} belonging to the fin-line structure which uses a dielectrically uniaxial substrate is examined. The two chosen substrate materials are boron nitride and sapphire with the physical dimensions of the housing being the same as those used above. A very interesting behavior can be observed from the numerical results which are plotted in Fig. 4. In the case of a fin-line printed on sapphire, the value of the effective dielectric constant increases with the rotation angle, while for the boron nitride substrate the opposite is true.

Finally, to demonstrate the flexibility of the theory presented in this paper, the propagation properties of bilateral fin-lines using more general anisotropic media are computed. The medium permeability is now characterized by a second rank tensor whose elements are given by $\mu_{xx} = \mu_2 \sin^2(\varphi) + \mu_1 \cos^2(\varphi)$, $\mu_{yy} = \mu_2 \cos^2(\varphi) + \mu_1 \sin^2(\varphi)$, $\mu_{zz} = \mu_3$, and $\mu_{xy} = \mu_{yx} = (\mu_2 - \mu_1) \sin(\varphi) \cos(\varphi)$. In this case, variables φ, μ_1, μ_2, and μ_3 are the analoges of θ, ϵ_1, ϵ_2, and ϵ_3, respectively. Fig. 5 illustrates how the normalized wavelength λ_n reacts to the addition of the magnetic anisotropy. The substrate material parameters used in computations were $\epsilon_1 = 8.7$, $\epsilon_2 = 9.6$, $\epsilon_3 = 11.4$, $\mu_1 = 1.0$, $\mu_2 = 1.6$, and $\mu_3 = 1.8$. The calculated data indicates that the presense of the $[\mu]$ tensor effectively shortens the normalized wavelength of the fin-line considerably. This effect can be seen for both diagonal ($\varphi = 0°, 90°$) as well as non-diagonal ($\varphi = 45°$) permeability tensor, wherein, for this set, all results were obtained at the center frequency of the *Ka*-band.

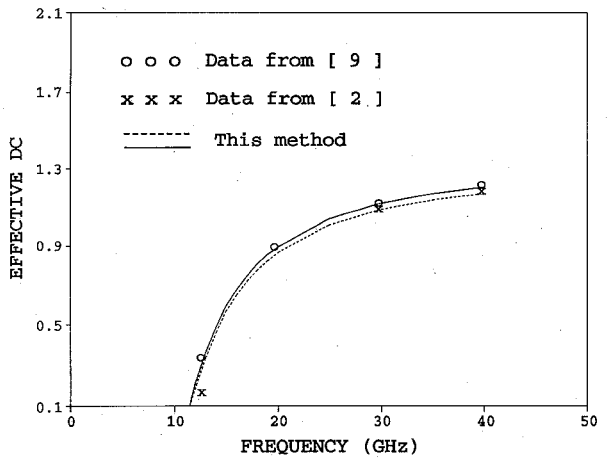

Fig. 2. Effective dielectric constant of the bilateral fin-line with $a = 7.112$ mm, $b = 3.556$ mm, $h_1 = 0.0625$ mm, $h_2 = 3.4935$ mm, $w = 0.5$ mm on isotropic substrate with $\epsilon_1 = \epsilon_2 = \epsilon_3 = 3.75$ and $\mu_1 = \mu_2 = \mu_3 = 1.0$, and dielectrically uniaxial substrate with $\epsilon_1 = \epsilon_3 = 3.0$, $\epsilon_2 = 3.5$, and $\mu_1 = \mu_2 = \mu_3 = 1.0$.

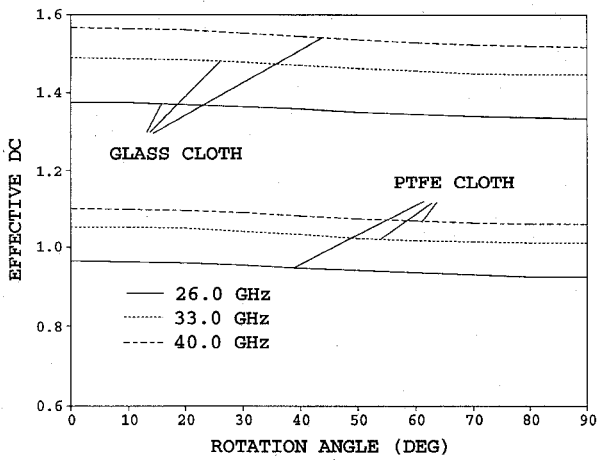

Fig. 3. Effective dielectric constant versus θ of the bilateral fin-line on PTFE and glass cloths with $a = 7.112$ mm, $b = 3.556$ mm, $h_1 = 0.0625$ mm, $h_2 = 3.4935$ mm, $w = 0.5$ mm.

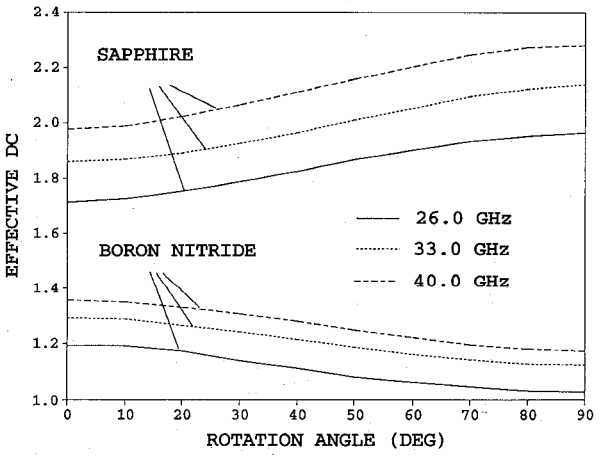

Fig. 4. Effective dielectric constant versus θ of the bilateral fin-line on boron nitride and sapphire with $a = 7.112$ mm, $b = 3.556$ mm, $h_1 = 0.0625$ mm, $h_2 = 3.4935$ mm, $w = 0.5$ mm.

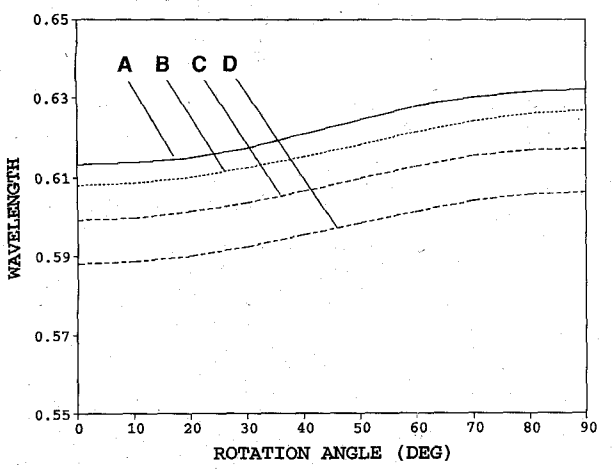

Fig. 5. Normalized wavelength versus θ as a function of φ of the bilateral fin-line on general anisotropic substrate with $a = 7.112$ mm, $b = 3.556$ mm, $h_1 = 0.0625$ mm, $h_2 = 3.4935$ mm, $w = 0.15$ mm, $\epsilon_1 = 8.7$, $\epsilon_2 = 9.6$, $\epsilon_3 = 11.4$, $\mu_1 = 1.0$, $\mu_2 = 1.6$, and $\mu_3 = 1.8$, and $f = 33.0$ GHz. (a) $[\epsilon]$ only. (b) $[\epsilon]$ and $[\mu]\varphi = 0°$. (c) $[\epsilon]$ and $[\mu]\varphi = 45°$. (d) $[\epsilon]$ and $[\mu]\varphi = 90°$.

IV. Conclusion

A full-wave analysis based on the spectral-domain technique of bilateral fin-lines on anisotropic substrates was presented. The formulation of the Green's function was carried out in the discrete Fourier transformed domain. Both the magnetic and dielectric anisotropy effects on bilateral fin-lines were examined to illustrate the usefulness of the newly derived Green's function for this structure. The dispersion properties were computed for several substrate materials as a function of the misalignment, and it was found that in some cases they can be greatly affected by the rotation of the coordinate axes. These generalized expressions may also be used to study the propagation characteristics of other transmission line structures, besides the bilateral fin-line, when they are printed on dielectric, magnetic, as well as mixed anisotropic media.

Appendix

The dyadic Green's function elements appearing in (9) are defined below

$$\tilde{G}_{yy}(\alpha, \beta) = \delta_1/\Psi^2 + \{H_z^+\Psi^+ - H_z^-\Psi^-\}/\delta_2 \quad \text{(A1a)}$$

$$\tilde{G}_{yz}(\alpha, \beta) = \delta_3/\Psi^2 + \{-E_y^- H_z^+\Psi^+ + E_y^+ H_z^-\Psi^-\}/\delta_2 \quad \text{(A1b)}$$

$$\tilde{G}_{zy}(\alpha, \beta) = \delta_3/\Psi^2 + \{-H_y^+\Psi^+ + H_y^-\Psi^-\}/\delta_4 \quad \text{(A1c)}$$

$$\tilde{G}_{zz}(\alpha, \beta) = \delta_5/\Psi^2 + \{E_y^- H_y^+\Psi^+ - E_y^+ H_y^-\Psi^-\}/\delta_4 \quad \text{(A1d)}$$

$$\Psi^2 = \tan(\gamma_2 h_2), \quad \text{(A1e)}$$

$$\Psi^+ = \tan(\gamma_+ h_1), \quad \text{(A1f)}$$

$$\Psi^- = \tan(\gamma_- h_1) \quad \text{(A1g)}$$

with

$$\delta_1 = (k_o^2 - \beta^2)/\gamma_2 \quad \text{(A2a)}$$

$$\delta_2 = (E_y^+ - E_y^-)\mu_{zz} \quad \text{(A2b)}$$

$$\delta_3 = \alpha\beta/\gamma_2 \quad \text{(A2c)}$$

$$\delta_4 = (E_y^+ - E_y^-)\mu_{yy} \quad \text{(A2d)}$$

$$\delta_5 = (k_o^2 - \alpha^2)/\gamma_2 \quad \text{(A2e)}$$

$$E_y^+ = -\gamma_+^2\{-Z_4^{-1} + (Z_3Z_1Z_4 + Z_3^2Y_2)(Z_4^3 - Z_4^2Z_3Y_1 + Z_4Z_3^2Y_2)\} + \{-Z_2Z_4^{-1} - (Z_3^2Y_4Z_4 - Z_3^2Y_2Z_2) \cdot (Z_4^3 - Z_4^2Z_3Y_1 + Z_4Z_3^2Y_2)\} \quad \text{(A3a)}$$

$$E_y^- = -\gamma_-^2\{-Z_4^{-1} + (Z_3Z_1Z_4 + Z_3^2Y_2)(Z_4^3 - Z_4^2Z_3Y_1 + Z_4Z_3^2Y_2)\} + \{-Z_2Z_4^{-1} - (Z_3^2Y_4Z_4 - Z_3^2Y_2Z_2) \cdot (Z_4^3 - Z_4^2Z_3Y_1 + Z_4Z_3^2Y_2)\} \quad \text{(A3b)}$$

$$H_\alpha = \{1/[-j\beta\gamma_+(1 - \mu_{xy}\epsilon_{xx}\mu_{xx}^{-1}\epsilon_{yx}^{-1})]\} \cdot \{\gamma_+^2 - k_o^2\epsilon_{zz}\mu_d/\mu_{xx} + \alpha^2\mu_{yy}/\mu_{xx} + \beta^2\mu_{xy}\epsilon_{zz}/\mu_{xx}\epsilon_{yx} - E_y^+\alpha\beta\mu_{yy}/\mu_{xx} + E_y^+\alpha\beta\mu_{xy}\epsilon_{yy}/\mu_{xx}\epsilon_{yx}\} \quad \text{(A3c)}$$

$$H_\beta = \{1/[-j\beta\gamma_-(1 - \mu_{xy}\epsilon_{xx}\mu_{xx}^{-1}\epsilon_{yx}^{-1})]\} \cdot \{\gamma_-^2 - k_o^2\epsilon_{zz}\mu_d/\mu_{xx} + \alpha^2\mu_{yy}/\mu_{xx} + \beta^2\mu_{xy}\epsilon_{zz}/\mu_{xx}\epsilon_{yx} - E_y^-\alpha\beta\mu_{yy}/\mu_{xx} + E_y^-\alpha\beta\mu_{xy}\epsilon_{yy}/\mu_{xx}\epsilon_{yx}\} \quad \text{(A3d)}$$

$$H_z^+ = -j\alpha H_\alpha + \gamma_+ E_y^+ \quad \text{(A3e)}$$

$$H_z^- = -j\alpha H_\beta + \gamma_- E_y^- \quad \text{(A3f)}$$

$$H_y^+ = \mu_{yy}\mu_{xx}\mu_d^{-1}(-\gamma_+ + j\beta H_\alpha) \quad \text{(A3g)}$$

$$H_y^- = \mu_{yy}\mu_{xx}\mu_d^{-1}(-\gamma_- + j\beta H_\beta) \quad \text{(A3h)}$$

where γ_2 is the transverse wavenumber in the isotropic region. Parameters $\gamma_\pm$ are the corresponding wavenumbers in the anisotropic region, and they are obtained by solving the fourth-order characteristic equation using a technique similar to the one presented in [10].

References

[1] N. G. Alexopoulos, "Integrated circuit structures on anisotropic substrates," *IEEE Trans. Microwave Theory Tech.*, vol. MTT-33, pp. 847–881, Oct. 1985.

[2] H. Y. Yang and N. G. Alexopoulos, "Uniaxial and biaxial substrate effects of finline characteristics," *IEEE Trans. Microwave Theory Tech.*, vol. MTT-33, pp. 24–29, Jan. 1987.

[3] F. Medina and M. Horno, "Determination of Green's function matrix for multiconductor and anisotropic multidielectric planar transmission lines: a variational approach," *IEEE Trans. Microwave Theory Tech.*, vol. MTT-33, pp. 933–940, Oct. 1985.

[4] M. Geshiro, S. Yagi, and S. Sawa, "Analysis of slotlines and microstrip lines on anisotropic substrates," *IEEE Trans. Microwave Theory Tech.*, vol. 39, pp. 64–69, Jan. 1991.

[5] T. Q. Ho and B. Beker, "Spectral domain analysis of shielded microstrip lines on anisotropic substrates," *IEEE Trans. Microwave Theory Tech.*, vol. 39, pp. 1017–1021, June 1991.

[6] G. E. Mariki and C. Yeh, "Dynamic three-dimensional TLM analysis of microstriplines on anisotropic substrate," *IEEE Trans. Microwave Theory Tech.*, vol. MTT-33, pp. 789–799, Sept. 1985.

[7] T. Kitazawa and T. Itoh, "Asymmetrical coplanar waveguide with finite metallization thickness containing anisotropic media," *IEEE Trans. Microwave Theory Tech.*, vol. 39, pp. 1426–1433, Aug. 1991.

[8] J. L. Tsalamengas, N. K. Uzunoglu, and N. G. Alexopoulos, "Propagation characteristics of a microstrip line printed on a general anisotropic substrate," *IEEE Trans. Microwave Theory Tech.*, vol. MTT-33, pp. 941–945, Oct. 1985.

[9] L. P. Schmidt and T. Itoh, "Spectral domain analysis of dominant and higher order modes in fin-lines," *IEEE Trans. Microwave Theory Tech.*, vol. MTT-28, pp. 981–985, Sept. 1980.

[10] T. Q. Ho and B. Beker, "Effects of misalignment of propagation characteristics of transmission lines printed on anisotropic substrates," *IEEE Trans. Microwave Theory Tech.*, to be published.